

# A small molecule enhances RNA interference and promotes microRNA processing

Ge Shan<sup>1,6</sup>, Yujing Li<sup>1,6</sup>, Junliang Zhang<sup>2</sup>, Wendi Li<sup>1</sup>, Keith E Szulwach<sup>1</sup>, Ranhui Duan<sup>1</sup>, Mohammad A Faghihi<sup>3</sup>, Ahmad M Khalil<sup>3</sup>, Lianghua Lu<sup>2</sup>, Zain Paroo<sup>4</sup>, Anthony W S Chan<sup>1</sup>, Zhangjie Shi<sup>5</sup>, Qinghua Liu<sup>4</sup>, Claes Wahlestedt<sup>3</sup>, Chuan He<sup>2</sup> & Peng Jin<sup>1</sup>

Small interfering RNAs (siRNAs) and microRNAs (miRNAs) are sequence-specific post-transcriptional regulators of gene expression. Although major components of the RNA interference (RNAi) pathway have been identified, regulatory mechanisms for this pathway remain largely unknown. Here we demonstrate that the RNAi pathway can be modulated intracellularly by small molecules. We have developed a cell-based assay to monitor the activity of the RNAi pathway and find that the small-molecule enoxacin (Penetrex) enhances siRNA-mediated mRNA degradation and promotes the biogenesis of endogenous miRNAs. We show that this RNAi-enhancing activity depends on the trans-activation-responsive region RNA-binding protein. Our results provide a proof-of-principle demonstration that small molecules can be used to modulate the activity of the RNAi pathway. RNAi enhancers may be useful in the development of research tools and therapeutics.

RNAi is a well-conserved mechanism that uses small noncoding RNAs to silence gene expression post-transcriptionally<sup>1,2</sup>. Gene regulation by RNAi has been recognized as one of the major regulatory pathways in eukaryotic cells<sup>3</sup>. The endogenous small RNAs can shape diverse cellular pathways, including chromosome architecture, development, growth control, apoptosis and stem cell maintenance<sup>4</sup>.

RNAi operates via two post-transcriptional mechanisms: targeted mRNA degradation by siRNA and suppression of translation/degradation by miRNA. The RNAi mechanism has been co-opted by researchers and has achieved broad utility in gene-function analysis, drug-target discovery and validation, and therapeutic development<sup>5,6</sup>. Given the pivotal roles of endogenous small RNAs in diverse biological pathways and the broad application of RNAi in biology and medicine, understanding the mechanism of the RNAi pathway is of great importance.

Over the last several years, key protein components involved in the RNAi pathway have been identified; however, little is known about the regulation of the RNAi pathway itself. Here we describe a chemical biology approach to modulate the RNAi pathway and report the identification of a small molecule that enhances RNAi and promotes the biogenesis of miRNA by facilitating the interaction between trans-activation-responsive region RNA-binding protein (TRBP) and RNAs. Our results provide a proof-of-principle demonstration that small molecules can be used to understand what cellular factors affect the activity of the RNAi pathway.

## RESULTS

### A chemical screen to identify small molecules that enhance RNAi

To alter the activity and gain insight into the regulation of the RNAi pathway, we developed a reporter system to monitor RNAi activity. In this system, a stable cell line derived from human embryonic kidney (HEK293) cells, expressing a gene encoding 293-EGFP (enhanced green fluorescent protein), was infected with a lentivirus expressing a short hairpin RNA (shRNA) that is processed into siRNA specifically targeting EGFP mRNA (Fig. 1a)<sup>7</sup>. The transduction led to reduced levels of EGFP in 293-EGFP cells; these cells are called RNAi-293-EGFP in the experiments following. To verify that the siRNAs against EGFP reduced EGFP expression, we transfected the clones with 2-O-methyl-RNAs, which has been shown to block the activity of the lentivirus-encoded EGFP siRNA<sup>8</sup>, and we observed increased GFP expression (Fig. 1a). To reduce variation between experiments, we isolated individual cell clones with moderate reductions in GFP expression and used them to screen for both inhibitors and enhancers of the RNAi pathway.

Using this system, we screened a collection of 2,000 US Food and Drug Administration-approved compounds and natural products and identified a small molecule named enoxacin that enhanced siRNA-mediated mRNA degradation. This small molecule was enoxacin (Fig. 1a). Enoxacin increased siGFP-mediated gene knockdown mediated by siRNA against EGFP in our cell-based reporter system in a dose-dependent manner, with a median effective concentration (EC<sub>50</sub>) of ~30 μM, whereas it had no effect on the

<sup>1</sup>Department of Human Genetics, Emory University School of Medicine, 615 Michael St., Atlanta, Georgia 30322, USA. <sup>2</sup>Department of Chemistry, The University of Chicago, 929 East 57th St., Chicago, Illinois 60637, USA. <sup>3</sup>Department of Molecular and Integrative Neurosciences, The Scripps Research Institute, 5353 Parkside Drive, Jupiter, Florida 33458, USA. <sup>4</sup>Department of Biochemistry, University of Texas Southwestern Medical Center, 5323 Harry Hines Blvd., Dallas, Texas 75390, USA. <sup>5</sup>The College of Chemistry, Peking University, 202 Chengfu Rd., Beijing, 100871, P.R. China. <sup>6</sup>These authors contributed equally to this work. Correspondence should be addressed to P.J. (pjin@genetics.emory.edu).

Received 8 January; accepted 24 June; published online 20 July 2008; doi:10.1038/nbt.1481

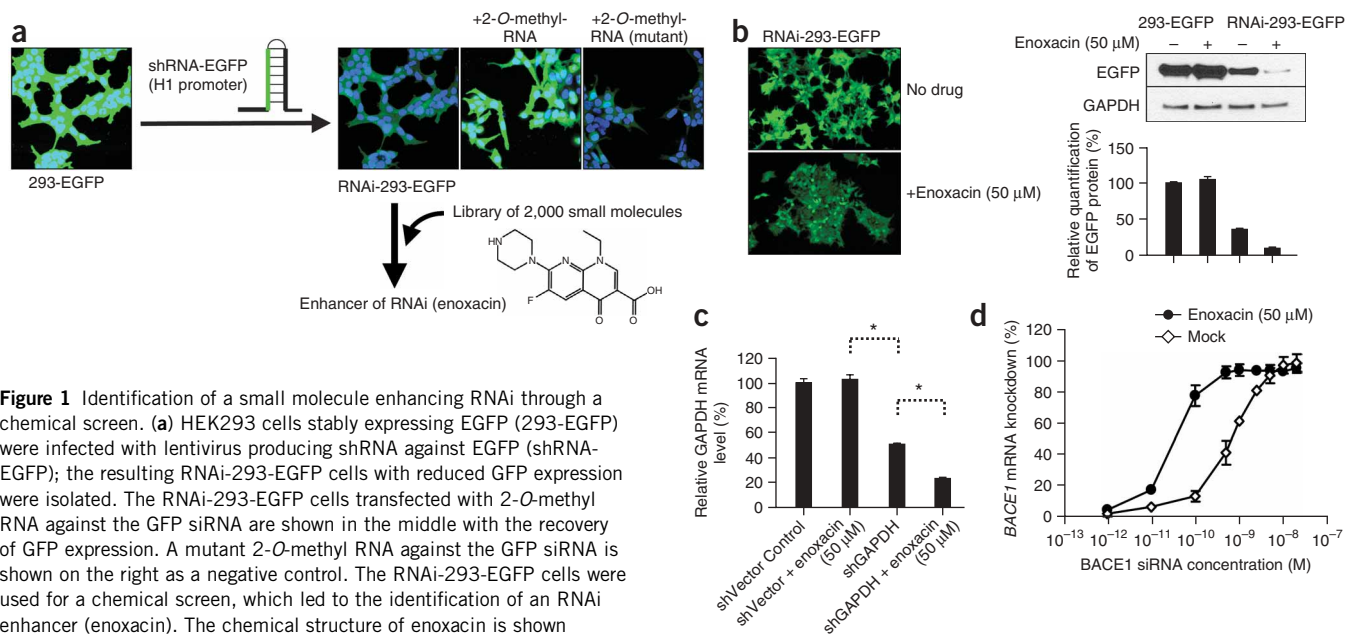


**Figure 1** Identification of a small molecule enhancing RNAi through a chemical screen. **(a)** HEK293 cells stably expressing EGFP (293-EGFP) were infected with lentivirus producing shRNA against EGFP (shRNA-EGFP); the resulting RNAi-293-EGFP cells with reduced GFP expression were isolated. The RNAi-293-EGFP cells transfected with 2-*O*-methyl RNA against the GFP siRNA are shown in the middle with the recovery of GFP expression. A mutant 2-*O*-methyl RNA against the GFP siRNA is shown on the right as a negative control. The RNAi-293-EGFP cells were used for a chemical screen, which led to the identification of an RNAi enhancer (enoxacin). The chemical structure of enoxacin is shown on the right. **(b)** Enoxacin enhances shRNA-EGFP-mediated gene silencing. The GFP protein levels were detected by western blot analysis using anti-EGFP antibody (right), with GAPDH as a loading control. The quantification is shown below. Fluorescence images of RNAi-293-EGFP cells without (top) or with (bottom) enoxacin are shown on the left (exposure time is different from panel **a**). Values are mean  $\pm$  s.d. **(c)** Enoxacin enhances shGAPDH-mediated gene silencing. Relative GAPDH mRNA levels in cells are determined by quantitative RT-PCR. Values are mean  $\pm$  s.d. for triplicate samples. \*,  $P < 0.001$ . **(d)** Enoxacin potentiates synthetic siRNA-induced knockdown of *BACE1*. Synthetic siRNA against human *BACE1* was transfected at a range of concentrations, from 1 pM to 20 nM, in HEK293FT cells. Knockdown of *BACE1* mRNA was graphed as a percentage of mock-treated samples in the presence or absence of enoxacin. Values are mean  $\pm$  s.d. for triplicate samples.

cells expressing GFP only (Fig. 1b and Supplementary Fig. 1). Importantly, enoxacin was relatively nontoxic, even at the high concentration of 150  $\mu$ M, which is lower than a clinical dose<sup>9</sup>. Similar enhancement of gene knockdown mediated by GAPDH-specific shRNA (shGAPDH) in cells stably expressing an shGAPDH was also observed upon enoxacin treatment (Fig. 1c). We also tested other shRNAs against GFP (different from the GFP used in our reporter system), luciferase and Fmr1, and again observed comparable increases (Supplementary Fig. 2), indicating that the effect of enoxacin on RNAi is indeed universal.

There are currently two means of harnessing the RNAi machinery to induce specific suppression of gene expression in cells: shRNAs and siRNA duplexes. Hence we also questioned whether enoxacin would have any effect on siRNA duplex-induced RNAi<sup>10</sup>. We found that enoxacin consistently gave rise to a left-shift of the concentration-response curve to an siRNA specifically targeting human *BACE1* mRNA (Fig. 1d). Importantly, the levels of unrelated transcripts, such as those encoding PINK-1 and actin, were not changed, suggesting that enoxacin did not induce nonspecific effects (data not shown). We also observed similar enhancement of knockdown efficiency by enoxacin using siRNA duplexes against different genes in various cell lines (Fig. 2). Furthermore, by comparing the gene knockdown efficiency among different concentrations of siRNA duplex used for transfection, we found that enoxacin substantially reduced the siRNA dosage required to achieve comparable knockdown efficiency (Figs. 1d and 2). These data together suggest that the small-molecule enoxacin enhances RNAi induced by either shRNAs or siRNA duplexes and substantially reduces the dosage required to achieve gene knockdown in mammalian cells.

### RNAi-enhancing activity of enoxacin is structure dependent

Enoxacin belongs to a family of synthetic antibacterial compounds based on a fluoroquinolone skeleton<sup>11</sup>. Fluoroquinolones have a broad antimicrobial spectrum and are very successful at treating a variety of bacterial infections<sup>12</sup>. As a family, fluoroquinolones target bacterial type II topoisomerases, such as DNA gyrase in Gram-negative bacteria and DNA topoisomerase IV in Gram-positive bacteria<sup>13</sup>; these agents do not inhibit eukaryotic topoisomerase II. Enoxacin has been used to treat bacterial infections ranging from gonorrhea to urinary tract infections<sup>14</sup>. Clinically, side effects have been minimal in adults<sup>14</sup>.

To test whether the quinolone family in general acts to enhance the RNAi pathway, we examined the effects of several other quinolones, both commercially available and synthetically modified molecules (enoxacin-V1-3), using our RNAi GFP reporter system (Fig. 3a). We found that two of these compounds (ciprofloxacin (Cipro) and norfloxacin (Noroxin)) have substantial RNAi-enhancing activity; however, these two molecules are less effective than enoxacin itself (Fig. 3b). Most other commercially available quinolones tested had either much less or almost no RNAi-enhancing activity. The addition of sterically blocking groups to the C-3 carboxylate (enoxacin-V1 and enoxacin-V3) and the piperazine terminal nitrogen atom of enoxacin (enoxacin-V2) reduced the RNAi-enhancing activity. Substitutions at the N-1, C-6 and C-7 positions of enoxacin also interfered with its RNAi-enhancing activity. The sensitivity of the RNAi-enhancing activity of enoxacin to chemical substitution suggests that it forms a specific complex distinct from the known targets of quinolones.

To exclude the possibility that enoxacin enhances RNAi activity by increasing the expression of one or more components in the RNAi pathway, we first examined the protein levels of multiple components in the RNA-induced silencing complex (RISC) and found no

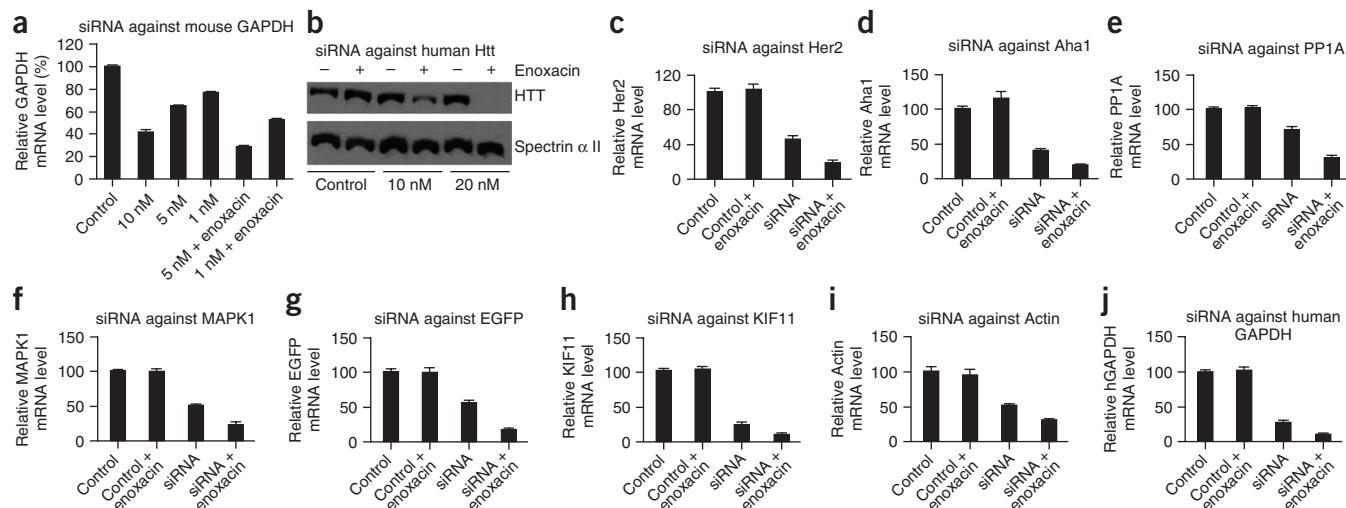


**Figure 2** Enoxacin potentiates additional synthetic siRNA-induced gene knockdown. **(a)** NIH3T3 cells were transfected with different amounts of siRNA duplexes against mouse GAPDH in the absence or presence of enoxacin. Relative GAPDH mRNA levels in the cells transfected with control and different dosages of siRNA are determined by quantitative RT-PCR. **(b)** 293 cells stably expressing Htt were transfected with 10 or 20 nM siRNA duplexes against human Htt in the absence or presence of enoxacin. The amounts of Htt are determined by western blot. **(c)** MCF-7 cells were transfected with 5 nM siRNA duplexes against human Her2 in the absence or presence of enoxacin. Relative Her2 mRNA levels are determined by TaqMan assay. **(d)** 293 cells were transfected with 5 nM siRNA duplexes against human Aha1 in the absence or presence of enoxacin. Relative Aha1 mRNA levels are determined by TaqMan assay. **(e)** 293 cells were transfected with 5 nM siRNA duplexes against human PP1A in the absence or presence of enoxacin. Relative PP1A mRNA levels are determined by TaqMan assay. **(f)** 293 cells were transfected with 5 nM siRNA duplexes against human MAPK1 in the absence or presence of enoxacin. Relative MAPK1 mRNA levels are determined by TaqMan assay. **(g)** 293-EGFP cells were transfected with 5 nM siRNA duplexes against EGFP in the absence or presence of enoxacin. Relative EGFP mRNA levels are determined by quantitative RT-PCR. **(h)** 293 cells were transfected with 5 nM siRNA duplexes against human KIF11 in the absence or presence of enoxacin. Relative KIF11 mRNA levels are determined by TaqMan assay. **(i)** HeLa cells were transfected with 20 nM siRNA duplexes against human actin in the absence or presence of enoxacin. Relative actin mRNA levels are determined by TaqMan assay. **(j)** 293 cells were transfected with 5 nM siRNA duplexes against human GAPDH in the absence or presence of enoxacin. Relative GAPDH mRNA levels are determined by TaqMan assay. In panels **a** and **c–j**, values are mean  $\pm$  s.d.

alteration in these levels in the cells treated with enoxacin (**Supplementary Fig. 3**). Because previous studies have shown that fluoroquinolones could massively increase or reduce steady-state levels of multiple mRNAs at a much higher concentration (250  $\mu$ M) than we used in this study (50  $\mu$ M), we further investigated the effect of

enoxacin on global gene expression<sup>15,16</sup>. We performed microarray analyses using both HEK293 and mouse NIH3T3 cells. Only a small number of genes (36 out of  $\sim$ 22,000 genes expressed in HEK293 cells and 10 out of  $\sim$ 20,000 genes expressed in NIH3T3 cells) displayed significant changes ( $>1.6$ -fold,  $P < 0.001$ ) in enoxacin-treated

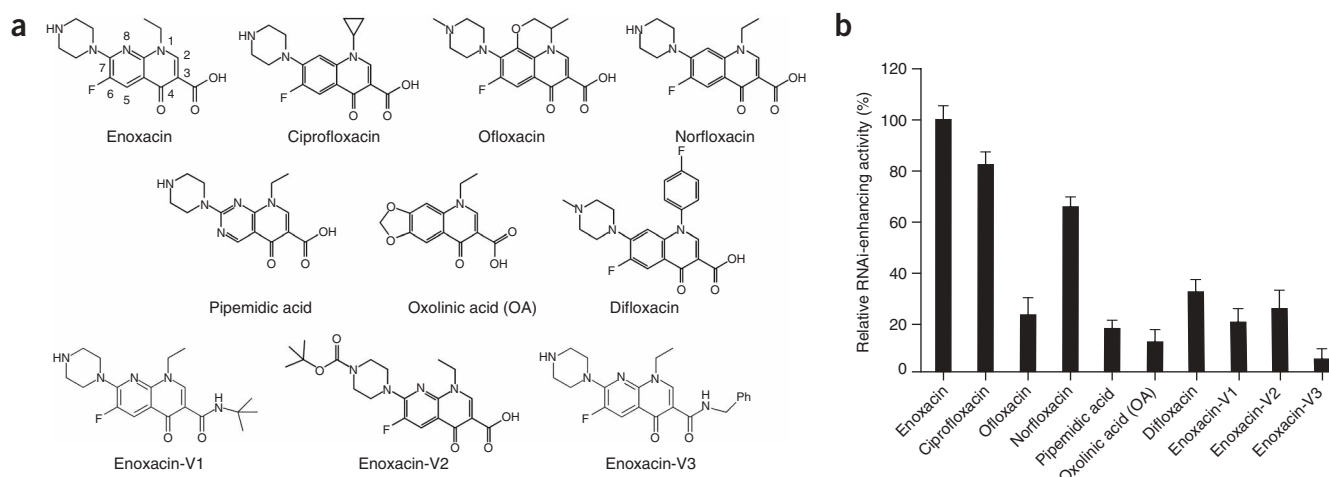
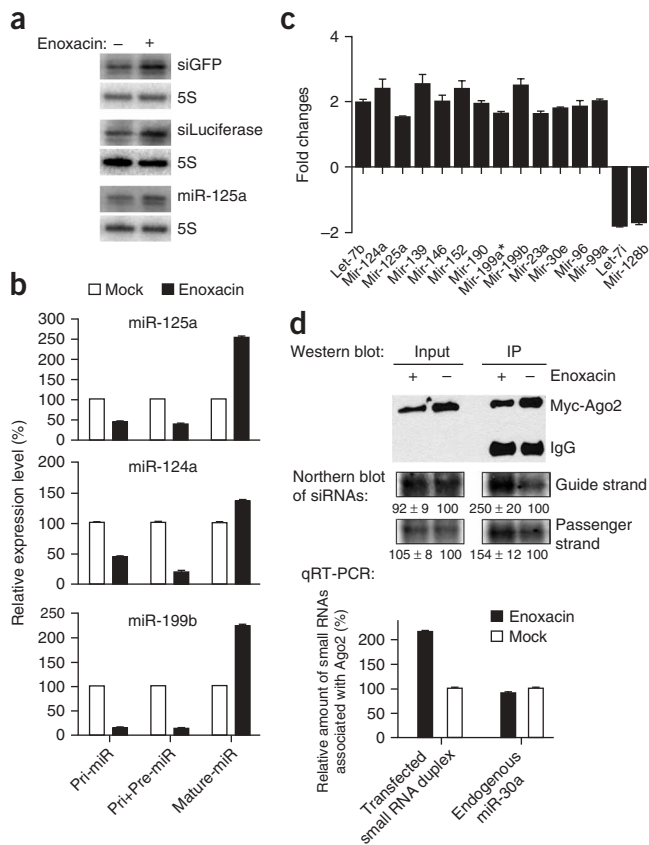


**Figure 3** Determination of chemical structure required for RNAi-enhancing activity. **(a)** The chemical structures of enoxacin variants are shown. **(b)** Relative RNAi-enhancing activities of enoxacin variants are shown. RNAi-enhancing activity was determined using RNAi-293-EGFP cells and fluorescence quantification on an Analyst HT plate reader. After subtraction of background fluorescence, the reduction of GFP fluorescence by enoxacin was set as 100%. Relative fluorescence intensity reductions measured in cells treated with the other compounds were normalized to the fluorescence reduction by enoxacin. Values are mean  $\pm$  s.d.



cells, and we were unable to find any gene consistently in both cell types (Supplementary Tables 1 and 2). These results suggest that the RNAi-enhancing activity we observed with enoxacin is not caused by pleiotropic effects on gene expression. We therefore hypothesized that enoxacin must interact specifically with the nucleic acids and protein(s) involved in the RNAi pathway to increase RNAi-enhancing activity.

#### Enoxacin promotes processing of miRNAs and loading of siRNAs

To determine the biological target(s) of enoxacin and the mechanism by which enoxacin modulates the RNAi pathway, we examined the expression of mature small RNAs in cells stably expressing either different shRNAs or the primary transcript of miR-125a (pri-miR-125a). We observed consistent increases in the expression of small RNAs in cells treated with enoxacin, despite the use of different promoters (Fig. 4a and Supplementary Fig. 4). Furthermore, we found that the addition of enoxacin led to increases in the mature form of miR-125a and corresponding decreases in the level of pri-miR-125a alone, as well as decreases in the total level of pri-miR-125a and precursor miR-125a (pre-miR-125a) (Fig. 4a–b and Supplementary Fig. 5). This suggests that enoxacin can promote the processing of miR-125a. The shGFP used in our initial reporter system mimics pre-miRNAs; therefore, it is processed by Dicer, rather than Drosha, which processes pri-miRNAs to pre-miRNAs<sup>7</sup>. Furthermore, enoxacin exerted effects on the siRNA duplex, which likewise does not require Drosha<sup>4</sup>. These data suggest that enoxacin might function at the level of Dicer-mediated precursor processing and/or loading onto RISCs.

To examine the effect of enoxacin on endogenous miRNAs, we used miRNA TaqMan assays to monitor the profiles of 157 miRNAs in transfected HEK293 cells stably expressing pri-miR-125a. The majority

**Figure 4** Enoxacin promotes the processing of miRNAs and the loading of siRNA duplexes onto RISCs. **(a)** Northern blots show that enoxacin enhances the level of siRNAs and mature miR-125a in cells transfected with shRNA against GFP, luciferase and miR-125a plasmids, respectively. 5S RNA was used as loading control. **(b)** Quantitative RT-PCR was used to measure the levels of pri-, pre- and mature forms of miR-125a, miR-124a and miR-199b in mock- and enoxacin-treated (50  $\mu$ M) HEK293 cells. Values are mean  $\pm$  s.d. for triplicate samples. **(c)** miRNAs with consistent changes in enoxacin-treated HEK293 cells (transfected HEK293 cells stably expressing pri-miR-125a were used). Each miRNA was examined by TaqMan MiRNA assay, and mock-treated cells are used as the baseline for all comparisons. The bar graph shows the average fold change with s.d. of the miRNAs that displayed consistent changes in triplicate experiments. **(d)** Top panel shows the western blot to detect the myc-Ago2 fusion protein in both input and immunoprecipitated complex (IP) using anti-myc antibody. Northern blots detecting the guide strand and passenger strand of siRNA duplexes are shown in the middle. (Note that different probes were used to detect the guide and passenger strands of siRNA duplexes, so the signal intensities appearing on the blot do not reflect the absolute amount of each strand.) The intensity of each band is quantified and indicated under the blot (untreated Input and untreated IP are 100). Bottom panel shows the relative amount of small RNAs associated with the immunoprecipitated Ago2-containing RISCs in the presence or absence of enoxacin (75  $\mu$ M), which was normalized to the inputs. Endogenous miR-30a that was not affected by enoxacin was used as a control (miR-30e shown in panel c is transcribed from a different genomic locus from miR-30a). Values are mean  $\pm$  s.d.

of endogenous miRNAs (142/157) were not significantly affected. Most of the miRNAs altered by enoxacin (13/15) had approximately twofold increases in expression of the mature form, whereas only two of the miRNAs had decreased levels of the mature forms (Fig. 4c). As with miR-125a, we also found decreased levels of the primary and precursor forms of the miRNAs whose mature forms increased in the presence of enoxacin (Fig. 4b and Supplementary Fig. 5). Interestingly, we noted that the precursor forms of the elevated endogenous miRNAs are generally abundant in untreated HEK293 cells, whereas the endogenous miRNAs that are not significantly affected by enoxacin generally have very little or undetectable precursor in cells (Supplementary Table 3). Furthermore, enoxacin treatment could increase the production of mature small RNAs from the miR-30a-based shRNAs (pre-miRNA-like RNAs) that were abundant in cells, whereas enoxacin had no effect on endogenous miR-30a, which had no detectable steady-state precursor form in cells (Fig. 4a; siLuciferase and data not shown). These data suggest that enoxacin could promote the processing of pre-miRNAs. This enhancement, mediated by enoxacin, depends largely on the amount of precursor RNAs in cells, rather than specific RNA sequences.

We also determined the effect of enoxacin on the stability and loading of siRNA duplexes onto RISC. It has been shown that Argonaute2 (Ago2) is a key component of the RISC responsible for mRNA cleavage activity (Slicer activity)<sup>17,18</sup>. We isolated Ago2-containing RISCs through immunoprecipitation from HEK293 cells transfected with siRNA duplexes and determined the amounts of siRNAs associated with Ago2 in the presence or absence of enoxacin using quantitative RT-PCR. The addition of enoxacin had no effect on the amount of siRNAs in the input, suggesting that enoxacin does not simply enhance the stability of siRNAs *in vivo* (Fig. 4d). With a similar amount of Ago2 protein immunoprecipitated, the amount of transfected siRNAs associated with Ago2-containing RISCs increased twofold upon treatment with enoxacin, whereas endogenous miR-30a, which is not altered by enoxacin, showed no difference (Fig. 4d, top and bottom panels).

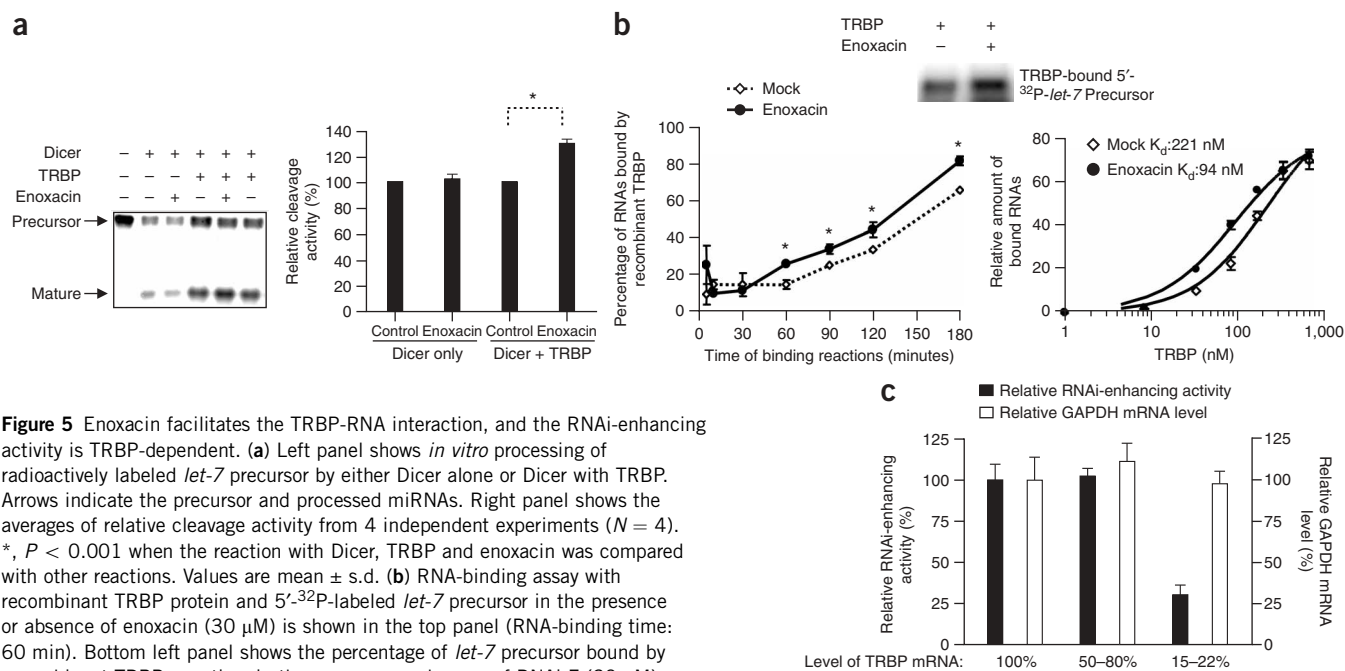


**Figure 5** Enoxacin facilitates the TRBP-RNA interaction, and the RNAi-enhancing activity is TRBP-dependent. **(a)** Left panel shows *in vitro* processing of radioactively labeled *let-7* precursor by either Dicer alone or Dicer with TRBP. Arrows indicate the precursor and processed miRNAs. Right panel shows the averages of relative cleavage activity from 4 independent experiments ( $N = 4$ ). \*,  $P < 0.001$  when the reaction with Dicer, TRBP and enoxacin was compared with other reactions. Values are mean  $\pm$  s.d. **(b)** RNA-binding assay with recombinant TRBP protein and 5'-<sup>32</sup>P-labeled *let-7* precursor in the presence or absence of enoxacin (30  $\mu$ M) is shown in the top panel (RNA-binding time: 60 min). Bottom left panel shows the percentage of *let-7* precursor bound by recombinant TRBP over time in the presence or absence of RNAi-E (30  $\mu$ M). \*,  $P < 0.001$ . Bottom right panel shows the percentage of *let-7* precursor bound by recombinant TRBP versus log of the protein concentration in the presence or absence of enoxacin (30  $\mu$ M). Values are mean  $\pm$  s.d. **(c)** The RNAi-enhancing activity is TRBP dependent. The siRNAs against TRBP were transfected into the cells stably expressing shGAPDH used in **Figure 1c** in the presence or absence of enoxacin (50  $\mu$ M). The reduction of TRBP had no effect on shGAPDH-mediated mRNA degradation because the GAPDH mRNA level remained unchanged in the absence of enoxacin. The correlation between TRBP mRNA level and RNAi-enhancing activity is shown. Values are mean  $\pm$  s.d.

Because quantitative RT-PCR could not distinguish between guide strands bound to Ago2 as a single strand or as part of an siRNA duplex, we performed northern blot analysis using the same immunoprecipitated RNAs to determine the amounts of both guide-strand and passenger-strand siRNAs associated with Ago2 (**Fig. 4d**, middle panel). Upon addition of enoxacin, both guide and passenger strands associated with Ago2 increased. Interestingly, the relative ratio between guide and passenger strands associated with Ago2 also increased by 30% in the presence of enoxacin, which suggests that enoxacin could promote the loading of siRNA duplexes onto RISCs.

### RNAi-enhancing activity is TRBP dependent

Dicer and TRBP play critical roles in the processing and loading of miRNAs and siRNAs onto the RISC<sup>19-22</sup>. We next examined whether enoxacin might be involved in the processing mediated by Dicer and TRBP using an established *in vitro* processing assay. Enoxacin had no effect on the processing of pre-*let-7* or pre-miR-30a by Dicer alone. However, the addition of enoxacin could enhance the processing of *let-7* or pre-miR-30a by Dicer and TRBP together (**Fig. 5a** and **Supplementary Fig. 6**). This enhancement was not observed with the addition of oxolinic acid, which has much less RNAi-enhancing activity (**Fig. 3** and **Supplementary Fig. 7a**). This result indicated that enoxacin might target TRBP. Because TRBP binds to miRNA precursors and facilitates the processing and loading of miRNAs, we performed a series of RNA-binding assays to examine the effect of enoxacin on the interaction between TRBP and miRNA precursor. We found that the presence of enoxacin increased the binding affinity of TRBP for miRNA precursors; the  $K_d$  under normal conditions is 221 nM, whereas the  $K_d$  in the presence of enoxacin is 94 nM (**Fig. 5b** and **Supplementary Fig. 7b**). These results suggest that enoxacin

promotes the processing and loading of siRNAs/miRNAs onto RISCs by facilitating the interaction between TRBP and RNAs in mammalian cells.

To further confirm the role of TRBP in enoxacin-mediated RNAi-enhancing activity, we performed a series of RNAi experiments using different amounts of siRNA duplexes against TRBP. The siRNAs against TRBP were transfected into cells stably expressing a shRNA against GAPDH (**Fig. 1c**). We determined the RNAi-enhancing activity of enoxacin in the presence of different levels of TRBP mRNA using the knockdown level of GAPDH as readout. Merely reducing TRBP mRNA to 85% had no effect on shGAPDH-mediated mRNA degradation (**Fig. 5c** and **Supplementary Table 4**); furthermore, the reduction of TRBP mRNA to 50–80% had no effect on RNAi-enhancing activity (**Fig. 5c** and **Supplementary Table 4**). However, when the TRBP mRNA level dropped below 22%, RNAi-enhancing activity was greatly reduced (**Fig. 5c** and **Supplementary Table 4**). These results together suggest that the RNAi-enhancing activity of enoxacin is TRBP dependent.

### Enoxacin enhances RNAi *in vivo*

To determine whether enoxacin has similar effects *in vivo*, we tested it in a GFP transgenic mouse line. When a lentivirus expressing shGFP (Lv-siGFP) is injected into these mice early in development, the construct knocks-down GFP expression<sup>7,23</sup>. However, injections of Lv-siGFP into adult mice did not alter GFP protein levels substantially (data not shown), possibly due to the stability of the GFP protein. We therefore chose to monitor the effects of enoxacin through measurements of GFP mRNA after targeted injections of Lv-siGFP in young pups. We chose mouse ears for the injections, because they are easily accessible; we could deliver the virus to a complete ear and

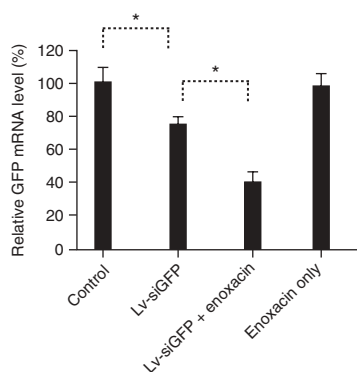


**Figure 6** Enoxacin enhances RNAi *in vivo*. The ears of GFP transgenic mice (*ACTB-EGFP*) were injected with shRNA-EGFP expressing lentivirus or Lv-siGFP, with or without enoxacin treatment (100  $\mu$ M). The relative GFP mRNA levels in the control ears injected with Lv-siGFP only, injected with both Lv-siGFP and enoxacin and injected with enoxacin alone are shown. \* $P < 0.001$  when Lv-siGFP is compared with control and Lv-siGFP+enoxacin is compared with Lv-siGFP alone.

obtain enough RNA from a single ear for quantitative RT-PCR analysis. In addition, we could compare the enoxacin-treated and enoxacin-untreated ears from the same mouse to reduce experimental variation. Three groups of injections were performed: Lv-siGFP alone, Lv-siGFP with enoxacin and enoxacin alone. We performed multiple rounds of injections in 10-day-old mice and found that Lv-siGFP alone reduced the GFP mRNA level to 80% of control tissues (20% knockdown). The addition of enoxacin enhanced the knockdown efficiency to 60% (40% GFP mRNA level remained), whereas enoxacin alone had no effect on GFP expression (Fig. 6), which is consistent with our previous cell culture data (Fig. 1b). These results suggest that enoxacin enhances siRNA-mediated mRNA degradation *in vivo*.

## DISCUSSION

Small noncoding RNAs play important roles in animal development, evolution and human disease<sup>3</sup>. Although our understanding of the mechanism of RNAi has dramatically increased with the identification of key proteins involved in the RNAi pathway, the modulation of this pathway in normal and disease states remains poorly understood, largely due to the overlapping, redundant and compensatory features of the biological pathways regulated by small RNAs<sup>10</sup>.

Chemical biology approaches that use small molecules to perturb protein networks of biological systems could be used to understand how the RNAi pathway is modulated. Using such an approach here, we identified a small molecule that enhances RNAi and promotes the biogenesis of miRNA by facilitating the interaction between TRBP and RNAs. Our results provide a proof-of-principle demonstration that small molecules can be used to study the RNAi pathway.

Enoxacin belongs to a family of synthetic antibacterial compounds, the fluoroquinolones<sup>11</sup>. Fluoroquinolones function as bacterial type II topoisomerase inhibitors<sup>11</sup>. To determine the specificity of enoxacin as an enhancer of RNAi, we also examined additional members of the fluoroquinolone family; only a select few of these compounds had substantial RNAi-enhancing activity, suggesting that the RNAi-enhancing activity does not depend on general fluoroquinolone activity, but rather on the unique chemical structure of enoxacin and a few related family members.

To further exclude the possibility that the RNAi-enhancing effect we observed is due to pleiotropic effects of enoxacin as a member of the fluoroquinolone family, which is known to alter gene expression at

a much higher concentration (250  $\mu$ M) than we used in this study (50  $\mu$ M), we examined genome-wide expression<sup>15,16</sup>. We observed very few genes with altered expression and found no genes that displayed consistent and substantial changes in the two cell lines tested in our assay. We did, however, find that the processing of those miRNAs whose precursors are abundant at steady state in cells was promoted by enoxacin. Previous studies have shown that overexpression of miRNAs could produce substantial changes in the mRNA levels<sup>24–26</sup>. However, in those studies the expression levels of specific miRNAs were elevated substantially, whereas in our assay we saw only a mild approximately twofold increase of mature miRNAs in the cells treated with enoxacin. Furthermore, how this mild increase of specific mature miRNAs affects the existing translational suppression remains to be studied in more detail. We have found that the twofold increase of specific mature miRNA had no effect on the translational suppression of corresponding reporter constructs (Supplementary Fig. 8). Overall, these results indicate that the RNAi-enhancing effect of enoxacin is specific.

Using a series of *in vitro* and *in vivo* analyses, we found that the enoxacin-mediated RNAi-enhancing activity is TRBP dependent, and enoxacin could facilitate the interaction between TRBP and RNAs. Furthermore, we found that enoxacin has no effect in an *in vitro* RISC-cleavage assay (Supplementary Fig. 9), which argues against the potential involvement of enoxacin in the step of mRNA-target recognition and cleavage. Rather, these results together suggest that enoxacin targets the step of RISC loading by enhancing the interaction between TRBP and RNAs. Indeed, it has been shown that the functionality of siRNAs is highly associated with the binding affinity of TRBP<sup>27</sup>; therefore the enhanced interaction between TRBP and RNAs mediated by enoxacin could be the basis of the RNAi-enhancing activity. Our results indicate that TRBP plays an important role(s) in modulating the activity or efficacy of siRNAs, and enoxacin potentially increases RISC loading efficiency and enhances RNAi by targeting TRBP-RNA interactions. In summary, we have developed a novel cell-based assay to monitor the activity of the RNAi pathway and identified a small molecule that enhances siRNA-mediated mRNA degradation and promotes the biogenesis of endogenous miRNAs. Our results suggest that chemical screens could provide a powerful route to understanding the modulation of the RNAi pathway. In addition, an RNAi enhancer could potentially facilitate the development of new RNAi tools and therapeutics.

## METHODS

**DNA constructs, siRNAs, cell lines and transfections.** Lv-siGFP was described previously<sup>7</sup>. The short hairpin vectors shLuciferase and shGAPDH were obtained from Open Biosystems. Details on other constructs and siRNA duplexes are described in Supplementary Methods. All cell lines, including HEK293, HeLa and NIH3T3, were cultured in DMEM with 10% FBS and penicillin/streptomycin. Plasmids, 2'-O-methyl-oligo siRNA and miRNA duplex were transfected into cells by Lipofectamine 2000 (Invitrogen). For *BACE1* siRNAs, the cells were trypsinized and reverse transfected with serial concentrations of *BACE1* siRNA (20 nM, 10 nM, 1 nM, 100 pM, 10 pM and 1 pM) using 0.2% Lipofectamine 2000 and the standard protocol. For siTRBP experiments, different concentrations of siTRBP (10 nM, 20 nM, 50 nM, 100 nM and 200 nM) were used. Stable cell lines were generated through selection using appropriate antibiotics. All the transfection experiments were repeated at least three times. For most of the experiments performed in this study, the final concentration of enoxacin is 50  $\mu$ M. Enoxacin was incubated with cells for 48 h before biological assays.

**Small-molecule screen, microscopy and fluorescent plate reading.** Based on the levels of GFP fluorescence intensity, individual clones of 293-EGFP-siGFP were isolated. Several clones were used for the chemical screen. Cells were

plated into 24-well plates. We added 2,000 individual drugs from The Spectrum Collection (10 mM in DMSO, MicroSource Discovery Systems) into individual wells at a final concentration of 50  $\mu$ M in 24 h. GFP fluorescence of each well was then visually inspected in 48 h using an inverted fluorescence microscope. Compounds that obviously changed EGFP fluorescence were chosen for follow-up study. Images were taken using LSM 510 confocal microscope (Zeiss). To quantify RNAi-enhancing activity, we measured EGFP fluorescence intensity in 48 h on an Analyst HT plate reader (Molecular Devices). An excitation filter at 485 nm and an emission filter at 520 nm were used with a dichroic mirror of 505 nm. To calculate an EC<sub>50</sub>, the maximum effect of RNAi enhancement was defined as the enoxacin effect at 100  $\mu$ M.

**Chemical synthesis.** Enoxacin and other fluoroquinolones tested here were purchased from Sigma. Enoxacin-V1, V2 and V3 were chemically synthesized as detailed in **Supplementary Methods**.

**Quantitative RT-PCRs, microarrays and western blot analyses.** Real-time PCR was performed with gene-specific primers and Power SYBR Green PCR Master Mix (Applied Biosystems) using a 7500 Fast Real-Time PCR system (Applied Biosystems). Profiling of mature miRNA expression was performed using Applied Biosystems' TaqMan miRNA assays with 8-plex reverse transcription and individual TaqMan miRNA real-time PCR assays according to protocols provided by the vendor. Gene expression profiles were evaluated using Affymetrix Expression Arrays, HG-U133\_Plus\_2 and Mouse430\_2. For western blotting, protein samples were separated on SDS-PAGE gels and then transferred to PVDF membranes (Millipore). Membranes were processed following the ECL western blotting protocol (Amersham). The details of these experiments are described in **Supplementary Methods**.

**Northern blot of small RNAs.** RNAs were isolated with TRIzol (Invitrogen), and then separated on 15% TBE urea gel, transferred and UV crosslinked to nylon membrane (Osmonics). <sup>32</sup>P-UTP-labeled probes were prepared with the Ambion mirVana miRNA Probe Construction Kit. Membranes were prehybridized at 65 °C for 1 h and hybridized for 12–16 h at 25 °C. Membranes were then washed three times at 25 °C and two times at 42 °C. Membranes were exposed and scanned with a Typhoon 9200 PhosphorImager (Amersham Biosciences).

**Determination of small RNA duplex loaded onto RISCs.** To quantify the transfected small RNA duplex loaded onto RISCs, we used the expression vector of Myc-Ago2 fusion protein and synthesized small RNA duplex. For ease of quantification, we used duplexes that resemble human miR-125a. In an earlier study we found that the expression of miR-125a in HEK293 cells is extremely low and could not be detected using either the MiRNA TaqMan assay or northern blot<sup>28</sup>. Briefly, HEK293FT ('fast transfect') cells were either transfected with Myc-tagged Ago2 plasmid or cotransfected with both Myc-tagged Ago2 expression vector and miR-125a duplexes (100  $\mu$ M) using Lipofectamine 2000. The transfected cells were split 24 h after transfection and treated with either no enoxacin or 75- $\mu$ M enoxacin for 48 h before collecting the cells for immunoprecipitation. The collected cells were lysed in lysis buffer containing 20 mM HEPES, pH 7.4, 10 mM NaCl, 1 mM MgCl<sub>2</sub>, 0.2 mM EDTA, 0.35% Triton-X100 (ref. 29) and 2 $\times$  protease inhibitor cocktail tablet (Roche) for 10 min. Ten percent of lysates were saved in 1 ml TRIzol for total RNA isolation as inputs. The remaining lysates were centrifuged at 20,000g for 20 min at 4 °C. Protein concentrations of the supernatants were quantified using Bradford Reagent (Bio-Rad). Lysates were adjusted to the concentrations of 1  $\mu$ g/ $\mu$ l, and 500  $\mu$ g total proteins were used for immunoprecipitation overnight at 4 °C using anti-Myc mAb (Invitrogen) together with Protein A Agarose Beads (Invitrogen). Immunoprecipitation beads were washed with the lysis buffer five times; 10% of the washed immunoprecipitation beads were used for western blots, and the remaining 90% for RNA extractions.

Input and immunoprecipitation RNAs were reverse transcribed with the High-Capacity cDNA Archive Kit (Applied Biosystems) combined with hsa-miR-125a- and has-mir30a-3p-specific primers (Applied Biosystems). Real-time PCR was conducted using TaqMan MicroRNA Assays specific for has-miR-30a-3p and has-miR-125a. Proteins extracted from the 10% immunoprecipitation beads and an equal amount of input

lysate proteins were separated by SDS-PAGE and probed with anti-Myc mAb to detect levels of Myc-tagged Ago2.

**Purification of recombinant TRBP.** His<sub>6</sub>-tagged TRBP was expressed in *Escherichia coli* BL21 (DE3) cells and purified with the Ni-NTA Fast Start Kit (Qiagen). The purity of the protein was analyzed by SDS-PAGE and its size was compared with a His-tagged standard (Invitrogen). Protein concentration was determined by Bradford Reagent Assay (Invitrogen).

**In vitro miRNA precursor processing assay and TRBP binding assay.** *Let-7* precursor RNA oligos were described previously and synthesized by Dharmacon (ref. 30). Human miR-30a precursor (GCGACUGUAAACAUCUC GACUGGAAGCUGUGAAGCCACAGAUGGGCUUUCAGUCGGAUGUUU GCAGCUGC) was synthesized by Dharmacon, as well. They were radioactively labeled at the 5' end with <sup>32</sup>P- $\gamma$ -ATP using T4 polynucleotide kinase (New England Biolabs). The labeled precursor was allowed to refold by heating at 95 °C for 2 min, followed by incubation at 37 °C for 1 h. For the processing assay, the labeled precursor was incubated with either Dicer or Dicer with TRBP in the buffer as described previously for 1 h<sup>22</sup>. The reaction was terminated and subjected to phenol/chloroform extraction and ethanol precipitation. Then the samples were separated on a 15% TBE urea gel, transferred and UV crosslinked to nylon membrane, which was then exposed for PhosphorImager scanning. Both unprocessed and processed precursors were quantified using Kodak MI software. The percentage of processed RNAs was used to calculate relative cleavage activity, with no enoxacin as a control (100%). Four independent experiments were performed and used to calculate mean and s.d.

TRBP and *let-7* precursor binding reactions were carried out in 1 $\times$  binding buffer (20 mM Tris-HCl, pH 8.0, 15 mM NaCl, 2.5 mM MgCl<sub>2</sub>) with 150 ng of purified recombinant TRBP and 10 ng <sup>32</sup>P-labeled *let-7* precursor in a total volume of 30  $\mu$ l with or without 30  $\mu$ M RNAi-E (or RNAi-E V5) at 30 °C for 5, 10, 30, 60, 90, 120 and 180 min. The reaction mixtures were then brought into contact with a UV lamp in a CL-1000 Ultraviolet Crosslinker (Stratagene) for 5 min on ice. After crosslinking, the samples were mixed with an equal volume of 2 $\times$  Gel Loading Buffer (Applied Biosystems) and incubated for 5 min at 95 °C. The denatured samples were separated onto 10% SDS-PAGE followed by gel dry using Gel Dryer (Fisher). The dried gels were exposed to Storage Phosphor Screen (Amersham Pharmacia Biotech) and the screens were scanned using a Typhoon 9200 PhosphorImager then quantified using Kodak MI software. The percentage of RNAs bound by TRBP was used to calculate the binding activity. At least four independent experiments were performed and used to calculate mean and s.d. For nitrocellulose filter binding assay, TRBP and *let-7* precursor binding reactions were carried out in 1 $\times$  binding buffer (20 mM Tris-HCl, pH 8.0, 15 mM NaCl, 2.5 mM MgCl<sub>2</sub>) with different amounts of purified recombinant TRBP and 10 ng <sup>32</sup>P-labeled *let-7* precursor in a total volume of 30  $\mu$ l with or without 30  $\mu$ M enoxacin at 30 °C for 60 min. Binding solutions were passed through MF-membrane filters (0.45 HA, Millipore) and washed with 4 ml of ice-cold wash buffer containing 50 mM Tris and 20 mM KCl (pH7.4). After the wash buffer was drained, the membranes were dried for 2 min at 25 °C. The dried membranes were immersed into ScintiVerse BD Cocktail (FLUKA), and liquid scintillation was counted using a LS6500 Multipurpose Scintillation Counter (Beckman). Data were plotted as relative amount of total RNA bound versus log of the TRBP concentration, and K<sub>d</sub> was determined with KaleidaGraph software (Synergy Software).

**Mice and lentiviral injection.** All animal procedures were performed based on protocols approved by Emory University Institutional Animal Care and Use Committee. The GFP transgenic line *C57BL/6-Tg(ACTB-EGFP)10sb/J* was obtained from The Jackson Laboratory. The lentivirus Lv-siGFP was produced as described previously<sup>7</sup>. Individual GFP transgenic mice (10 d old) were injected with the lentivirus Lv-siGFP (2  $\mu$ l) into either one ear (to demonstrate the effect of Lv-siGFP only) or both ears (for injection of enoxacin or control later) (day 10). Enoxacin or control solution (mock) (2  $\mu$ l) was then injected once a day for 3 consecutive days (days 12, 13 and 14) into one of the ears 2 d after Lv-siGFP injection. The concentration of injected enoxacin solution was 100  $\mu$ M. As a negative control, a group of mice were also injected with enoxacin or control solution into one ear. Mice were then killed (day 15), and the

ears were removed and used for RNA isolation and quantitative RT-PCR analysis of GFP mRNA. For each condition, at least six mice in three different groups were injected.

**Statistical methods.** We used single-factor ANOVA analysis to show significant differences between control and enoxacin treatment. We performed post-hoc *t*-tests (two-sample assuming equal variances) to determine significance and indicated *P* value.

*Note: Supplementary information is available on the Nature Biotechnology website.*

#### ACKNOWLEDGMENTS

We would like to thank S. Warren, S. Chang, K. Garber and C. Strauss for their helpful discussions and critical reading of the manuscript and H. Ju for technical assistance. We thank I. Verma, J. Belasco and G. Hannon for providing us the plasmids. Q.L. is a Damon Runyon Scholar (DRS-43) and is supported by the Welch Foundation (I-1608). P.J. is supported by NIH grants (NS051630 and MH076090). P.J. is the recipient of a Beckman Young Investigator Award and a Basil O'Connor Scholar Research Award and is an Alfred P. Sloan Research Fellow in Neuroscience.

#### AUTHOR CONTRIBUTIONS

P.J. designed the research. G.S. conducted the chemical screen and identified the small molecule presented in this paper. G.S. and Y.L. performed the majority of mechanistic experiments. J.Z., L.L., Z.S. and C.H. performed chemical synthesis. G.S., Y.L., W.L., M.A.F., A.M.K. and C.W. performed additional testing on the compound. K.E.S. and R.D. performed miRNA profiling and developed the reporter system. A.W.S.C., Z.P. and Q.L. provided some reagents used in this paper. G.S., Y.L. and P.J. wrote the paper.

#### COMPETING INTERESTS STATEMENT

The authors declare competing financial interests: details accompany the full-text HTML version of the paper at <http://www.nature.com/naturebiotechnology/>

Published online at <http://www.nature.com/naturebiotechnology/>

Reprints and permissions information is available online at <http://npg.nature.com/reprintsandpermissions/>

- Hannon, G.J. RNA interference. *Nature* **418**, 244–251 (2002).
- Bartel, D.P. MicroRNAs: genomics, biogenesis, mechanism, and function. *Cell* **116**, 281–297 (2004).
- Plasterk, R.H. Micro RNAs in animal development. *Cell* **124**, 877–881 (2006).
- Zamore, P.D. & Haley, B. Ribo-gnome: the big world of small RNAs. *Science* **309**, 1519–1524 (2005).
- Dykxhoorn, D.M. & Lieberman, J. The silent revolution: RNA interference as basic biology, research tool, and therapeutic. *Annu. Rev. Med.* **56**, 401–423 (2005).
- Dykxhoorn, D.M. & Lieberman, J. Running interference: prospects and obstacles to using small interfering RNAs as small molecule drugs. *Annu. Rev. Biomed. Eng.* **8**, 377–402 (2006).
- Tiscornia, G., Singer, O., Ikawa, M. & Verma, I.M. A general method for gene knockdown in mice by using lentiviral vectors expressing small interfering RNA. *Proc. Natl. Acad. Sci. USA* **100**, 1844–1848 (2003).
- Hutvagner, G., Simard, M.J., Mello, C.C. & Zamore, P.D. Sequence-specific inhibition of small RNA function. *PLoS Biol.* **2**, E98 (2004).
- Patel, S.S. & Spencer, C.M. Enoxacin: a reappraisal of its clinical efficacy in the treatment of genitourinary tract infections. *Drugs* **51**, 137–160 (1996).
- Pasquinelli, A.E. Demystifying small RNA pathways. *Dev. Cell* **10**, 419–424 (2006).
- Bhanot, S.K., Singh, M. & Chatterjee, N.R. The chemical and biological aspects of fluoroquinolones: reality and dreams. *Curr. Pharm. Des.* **7**, 311–335 (2001).
- Hopper, D.C. & Wolfson, J.S. *Quinolone Antimicrobial Agents* 3<sup>rd</sup> edn. (ASM Press, Washington, DC; 2003).
- Mitscher, L.A. Bacterial topoisomerase inhibitors: quinolone and pyridone antibacterial agents. *Chem. Rev.* **105**, 559–592 (2005).
- Schaeffer, A.J. The expanding role of fluoroquinolones. *Am. J. Med.* **113** Suppl 1A, 45S–54S (2002).
- Dalhoff, A. & Shalit, I. Immunomodulatory effects of quinolones. *Lancet Infect. Dis.* **3**, 359–371 (2003).
- Eriksson, E., Forsgren, A. & Riesbeck, K. Several gene programs are induced in ciprofloxacin-treated human lymphocytes as revealed by microarray analysis. *J. Leukoc. Biol.* **74**, 456–463 (2003).
- Rand, T.A., Ginalski, K., Grishin, N.V. & Wang, X. Biochemical identification of Argonaute 2 as the sole protein required for RNA-induced silencing complex activity. *Proc. Natl. Acad. Sci. USA* **101**, 14385–14389 (2004).
- Liu, J. *et al.* Argonaute2 is the catalytic engine of mammalian RNAi. *Science* **305**, 1437–1441 (2004).
- Bernstein, E., Caudy, A.A., Hammond, S.M. & Hannon, G.J. Role for a bidentate ribonuclease in the initiation step of RNA interference. *Nature* **409**, 363–366 (2001).
- Chendrimada, T.P. *et al.* TRBP recruits the Dicer complex to Ago2 for microRNA processing and gene silencing. *Nature* **436**, 740–744 (2005).
- Jiang, F. *et al.* Dicer-1 and R3D1-L catalyze microRNA maturation in *Drosophila*. *Genes Dev.* **19**, 1674–1679 (2005).
- Forstemann, K. *et al.* Normal microRNA maturation and germ-line stem cell maintenance requires Loquacious, a double-stranded RNA-binding domain protein. *PLoS Biol.* **3**, e236 (2005).
- Okabe, M., Ikawa, M., Kominami, K., Nakanishi, T. & Nishimune, Y. 'Green mice' as a source of ubiquitous green cells. *FEBS Lett.* **407**, 313–319 (1997).
- Jackson, A.L. *et al.* Widespread siRNA "off-target" transcript silencing mediated by seed region sequence complementarity. *RNA* **12**, 1179–1187 (2006).
- Lim, L.P. *et al.* Microarray analysis shows that some microRNAs downregulate large numbers of target mRNAs. *Nature* **433**, 769–773 (2005).
- Jing, Q. *et al.* Involvement of microRNA in AU-rich element-mediated mRNA instability. *Cell* **120**, 623–634 (2005).
- Katoh, T. & Suzuki, T. Specific residues at every third position of siRNA shape its efficient RNAi activity. *Nucleic Acids Res.* **35**, e27 (2007).
- Duan, R., Pak, C. & Jin, P. Single nucleotide polymorphism associated with mature miR-125a alters the processing of pri-miRNA. *Hum. Mol. Genet.* **16**, 1124–1131 (2007).
- Chu, C.Y. & Rana, T.M. Translation repression in human cells by microRNA-induced gene silencing requires RCK/p54. *PLoS Biol.* **4**, e210 (2006).
- Hutvagner, G. & Zamore, P.D. A microRNA in a multiple-turnover RNAi enzyme complex. *Science* **297**, 2056–2060 (2002).